

Supporting Information for
**Electronic promoter or reacting species? The role of LiNH₂ on Ru in catalyzing
NH₃ decomposition**

Jianping Guo,^{a,b} Zheng Chen,^c Anan Wu,^{*,c} Fei Chang,^{a,b} Peikun Wang,^{a,b} Daqiang Hu,^a Guotao Wu,^a Zhitao Xiong,^a Pei Yu,^{a,b} Ping Chen,^{*,a,d}

^aDalian Institute of Chemical Physics, Chinese Academy of Sciences, Dalian 116023, China.

^bUniversity of Chinese Academy of Sciences, Beijing 100049, China.

^cState Key Laboratory of Physical Chemistry of Solid Surfaces and College of Chemistry and Chemical Engineering, Xiamen University, Xiamen 361005, China.

^dState Key Laboratory of Catalysis, Dalian Institute of Chemical Physics, Chinese Academy of Sciences, Dalian 116023, China.

*Corresponding author: pchen@dicp.ac.cn, ananwu@xmu.edu.cn

Materials and Methods

Materials

LiNH₂ (Aldrich, 95.0%), RuCl₃·xH₂O (Aladdin, 97%), Lithium rod (Alfa Aesar, 99.9%), KNO₃ (Alfa Aesar, 99.0%), were used without further treatment. CNTs, having a mean diameter of 20 nm and BET surface area of 104 m² g⁻¹ were supplied by Professor H. B. Zhang's group in Chemistry Department, Xiamen University, China. NH₃ gas was purified by anhydrous CaO before used for catalytic test. As Li metal and LiNH₂ are sensitive to moisture and oxygen, sample preparation and loading were conducted in a glove box filled with Argon.

Preparation of Li₂NH. Li₂NH was prepared by heating commercial LiNH₂ at 773 K under vacuum for 5 hours.

Preparation of Ru-LiNH₂. A mixture of RuCl₃·xH₂O and LiNH₂ with a given weight

ratio was ball milled at 150 rpm in an agart jar at 323 K on a Retsch planetary ballmill (PM400) under Ar atmosphere for 3h. Then the solid residue was purified by stirring it in dry THF (30 ml) followed by centrifugation for 3 times to remove LiCl. The purified product was dried under vacuum and stored in glove box.

Preparation of MgO. MgO was obtained via thermal decomposition of $\text{MgC}_2\text{O}_4 \cdot 2\text{H}_2\text{O}$ in Ar flow according to reference.¹

Preparation of supported Ru catalysts. CNTs or MgO supported Ru catalysts were prepared by the incipient wetness impregnation of CNTs or MgO with acetone solution of $\text{RuCl}_3 \cdot x\text{H}_2\text{O}$.² The weight ratio of Ru to CNTs or MgO is *ca.* 0.05, respectively. Prior to test, the samples were reduced in H_2 (30 ml min^{-1}) at 673 K for 2 hours.

Preparation of K or LiNH_2 -promoted Ru/MgO catalysts. The K promoted-Ru/MgO catalyst was prepared by the dispersion of the prepared Ru/MgO in a KNO_3 aqueous solution, followed by drying in Ar. The atomic ratio of K/Ru in the catalyst is *ca.* 2.³ The LiNH_2 -Ru/MgO catalyst was prepared by impregnating the prepared Ru/MgO in an Li-ammonia solution. Li metal converted to LiNH_2 in the presence of Ru. The atomic ratio of Li to Ru is *ca.* 11.5:1.

Catalyst testing. Ammonia decomposition reactions were performed in a continuous-flow fixed-bed quartz reactor (inner diameter = 4 mm). Typically, 30 mg of catalyst or its precursor was loaded, and the temperature was raised at a ramping rate of 2 K min^{-1} . The gas composition was analyzed using on-line gas chromatograph (GC-2014C, Shimadzu) equipped with a Porapak N column, a 5A molecular sieve column and

TCD detector. Ammonia conversion data reported here were collected after 30 min time-on-stream at the corresponding temperature.

XANES and EXAFS measurements. Spectra at Ru K-edge were recorded at the BL14W beamline of Shanghai Synchrotron Radiation Facility (SSRF, electron energy of 3.5 GeV and ring currents of 300 mA). Samples were pressed into pellets and then sealed with KAPTON film on both sides to avoid air contamination.

XRD measurements. XRD patterns were recorded on a PANalytical X'pert diffractometer using a homemade sample cell covered with KAPTON film to avoid air contamination.

TG measurements. TG measurement was performed on a Netsch 449C TG unit. Small loading of *ca.* 5 mg was used. Argon was used as carrier gas and the ramping rate was set on 2K min⁻¹.

FTIR measurement. FTIR measurement was performed on a Varian 3100 unit in DRIFT mode. The resolution is 4 cm⁻¹.

Temperature-Programmed techniques. Temperature-programmed reactions were performed in a tubular quartz reactor and the exhaust gases were analyzed by an on-line mass spectrometer (Hiden HPR20). Samples were heated in a flow of Ar (30 ml min⁻¹) from room temperature to desired temperatures.

Computational details. All calculations were performed with the Vienna ab initio simulation package (VASP).⁴ Projector-augmented-wave (PAW) potentials⁵ were employed in connection with the PBE gradient-dependent exchange-correlation functions.⁶ An energy cutoff of 500 eV was used to guarantee a good convergence for

the total energies and forces. The convergence criterion for energy is 10^{-5} eV/atom. For the structural optimization, full relaxation of cell volume and atomic positions was performed until the forces were less than 0.01 eV/Å. A periodic slab of eight atomic layers (256 atoms for the pristine Li_2NH surface) were used to simulate the Li_2NH (110) surface, for which atoms in the bottom four layers were fixed. For the Brillouin zone integrations, the k points were chosen using a $3 \times 3 \times 1$ Monkhorst-Pack mesh.⁷

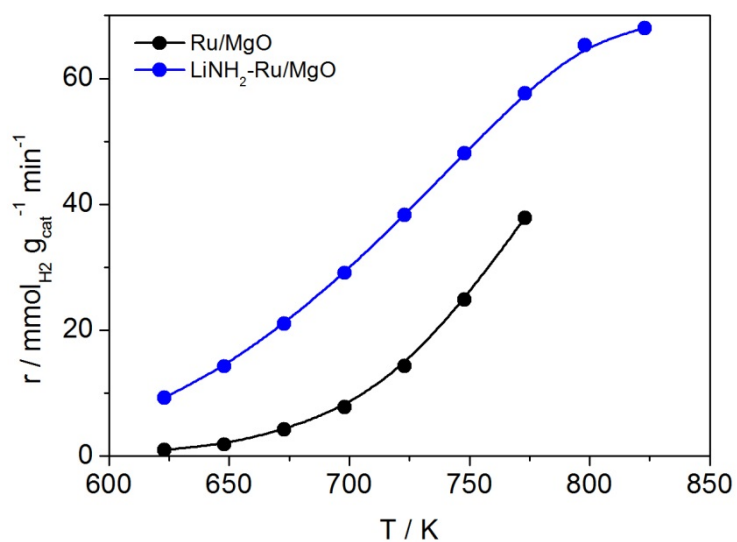


Figure S1. Temperature dependences of the activities of Ru-based catalysts under pure NH₃ flow with WHSV = 60,000 ml_{NH3} g_{cat}⁻¹ h⁻¹.

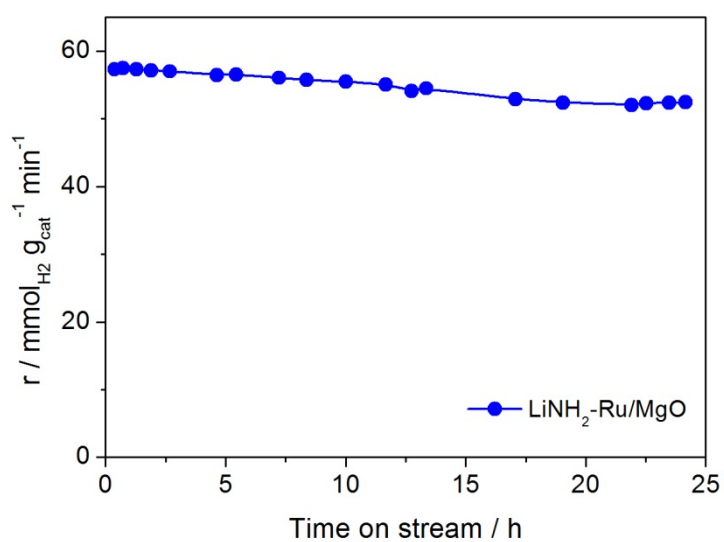


Figure S2. Stability test of the LiNH₂-Ru/MgO under pure NH₃ with WHSV = 60,000 ml_{NH3} g_{cat}⁻¹ h⁻¹ at 773 K.

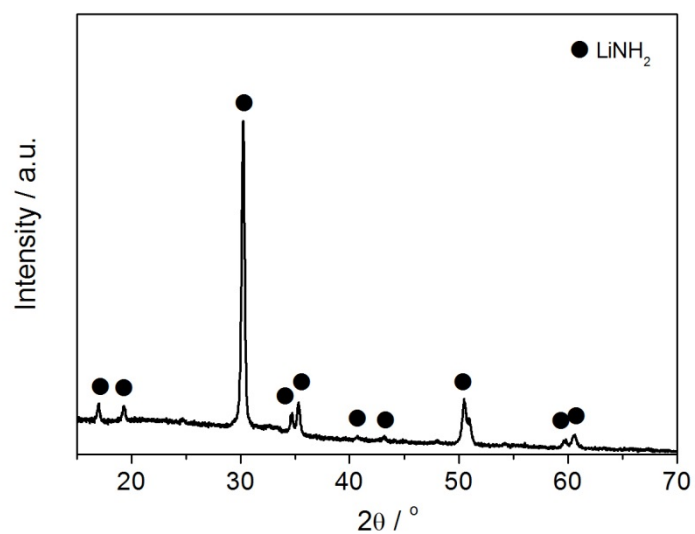


Figure S3. XRD pattern of as-prepared 5 wt% Ru-LiNH₂ sample.

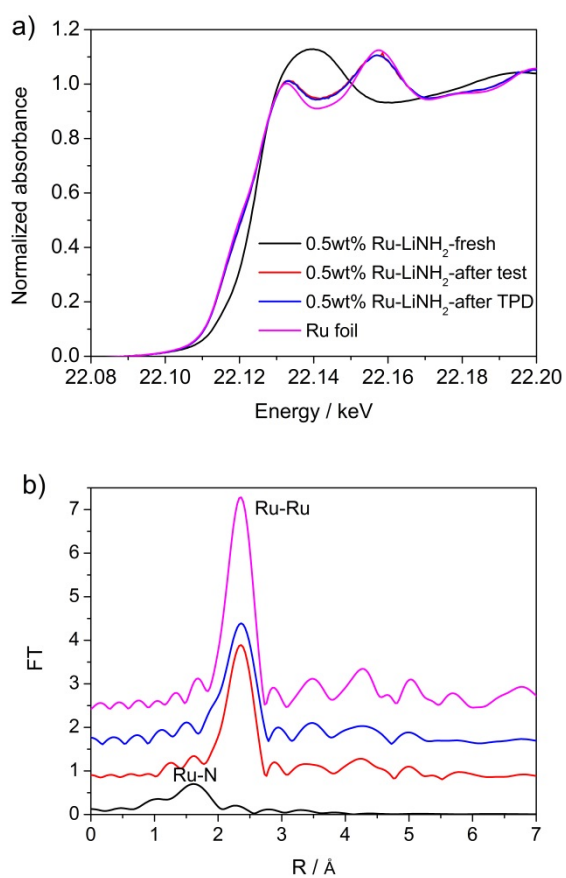


Figure S4. Ru K-edge XANES (a) and EXAFS (b) spectra of Ru-containing samples. To facilitate the measurement and to have uniform chemical state of Ru, 0.5 wt% Ru loading was adopted.

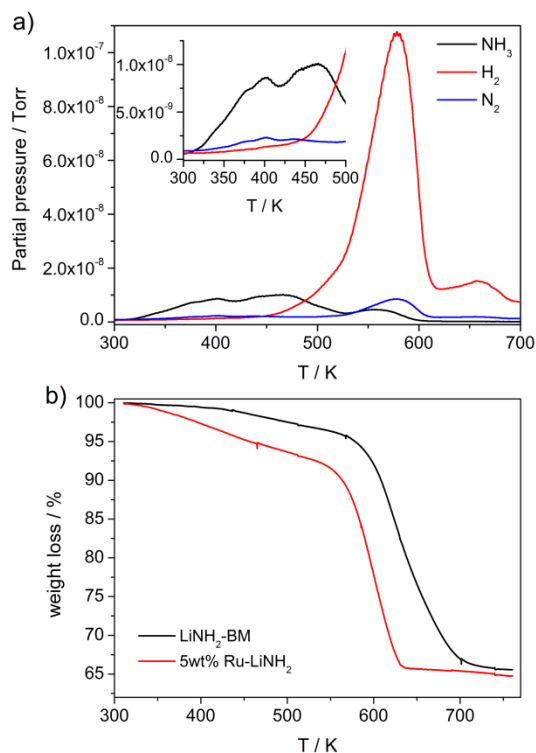


Figure S5. Characterization of the interaction of Ru and LiNH_2 . (a) Temperature-programmed-decomposition profile (TPD) of 5 wt% Ru- LiNH_2 , the inset is the enlarged portion of the temperature range of 300-500 K, and (b) TG measurements of 5 wt% Ru- LiNH_2 and LiNH_2 samples.

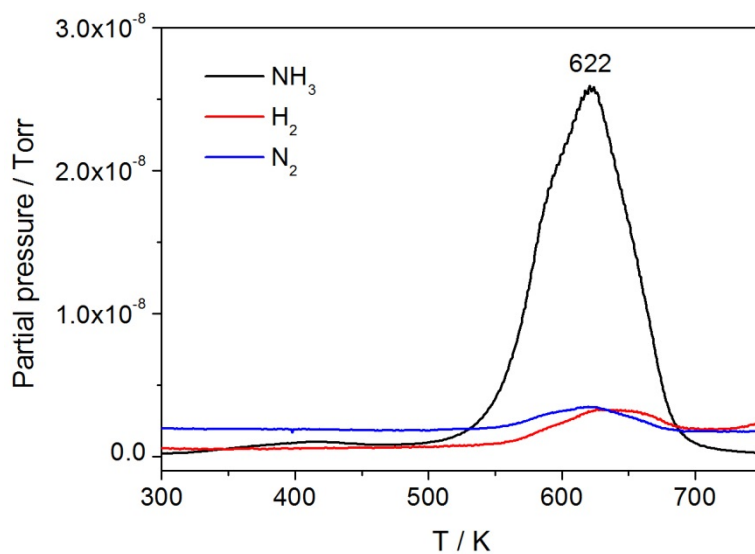


Figure S6. Temperature-Programmed-Decomposition (TPD) profile of LiNH_2 sample after ball milling. Reaction condition: sample loading – 20 mg, carrier gas – Ar, flow rate – 40 ml min^{-1} , ramping rate – 2 K min^{-1} .

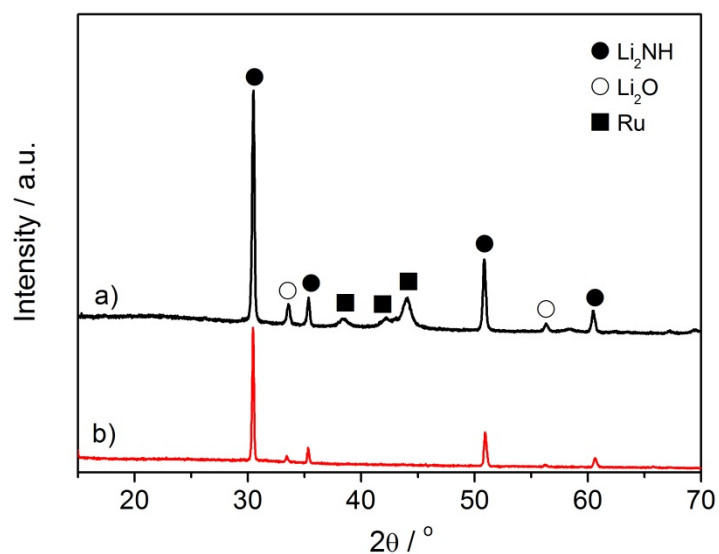


Figure S7. XRD patterns of post-TPD samples of 5 wt% Ru-LiNH₂ sample (a) and LiNH₂ (b). Reaction condition: sample loading – 20 mg, carrier gas – Ar, flow rate – 40 ml min⁻¹, heating to 723 K, ramping rate – 2K min⁻¹.

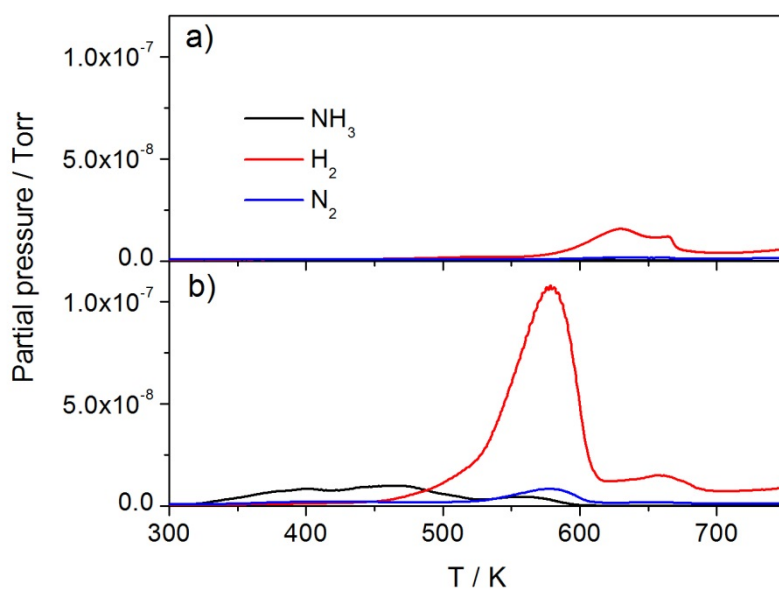


Figure S8. Temperature-Programmed-Decomposition (TPD) profiles of Ru-Li₂NH sample (a) prepared by ball milling Ru and Li₂NH with a molar ratio of 1:2, and 5 wt% Ru-LiNH₂ (b). Reaction condition: sample loading – 20 mg, carrier gas – Ar, flow rate – 40 ml min⁻¹, ramping rate – 2K min⁻¹.

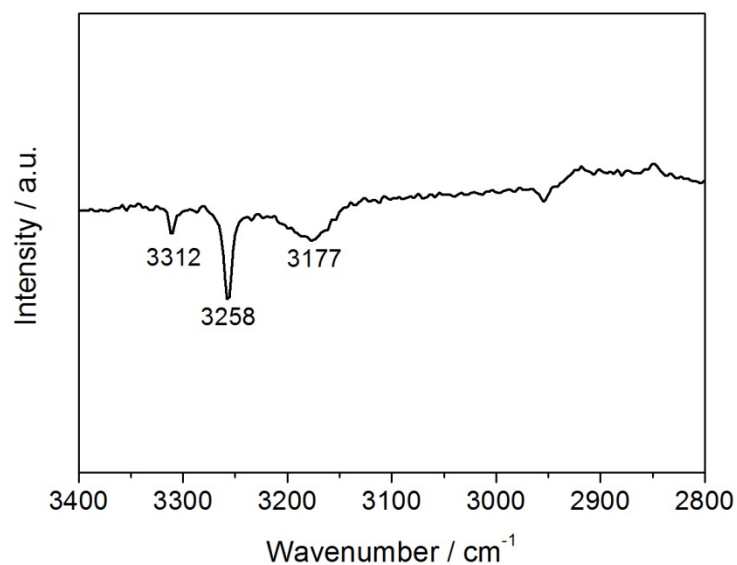


Figure S9. FTIR spectrum of LiNH₂-Ru/MgO after testing for decomposition of 5% NH₃/Ar. The sample was collected after reaction at 673 K followed by cooling rapidly to room temperature. The IR bands at 3258 and 3312 cm⁻¹ are stretching vibrations of LiNH₂ and the band at 3177 cm⁻¹ is the stretching vibration of Li₂NH.

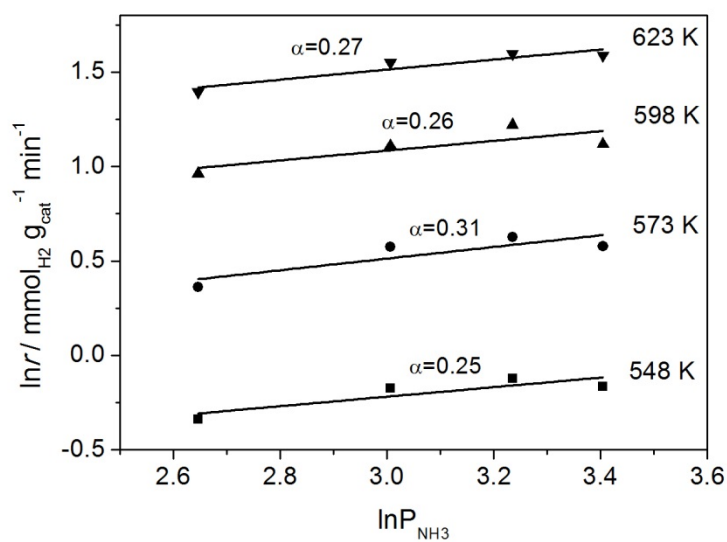
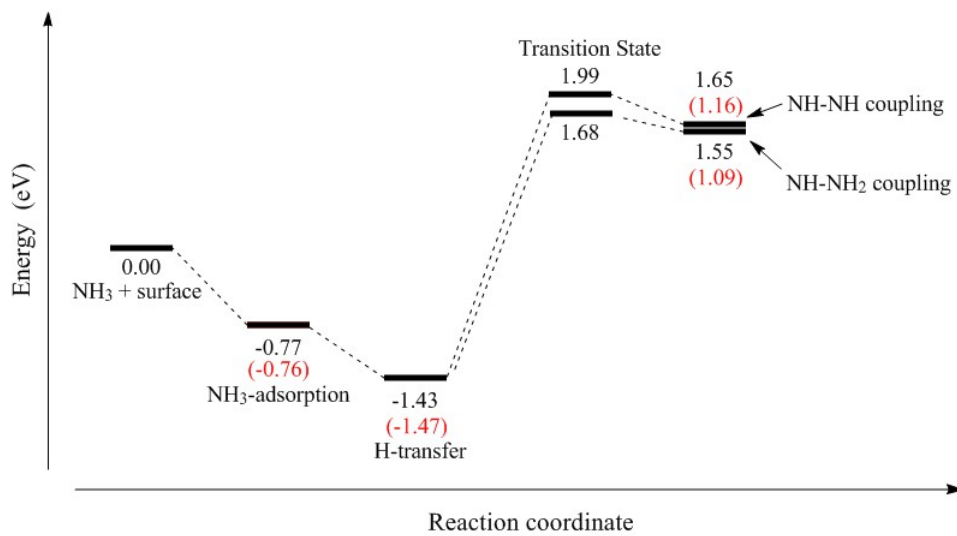
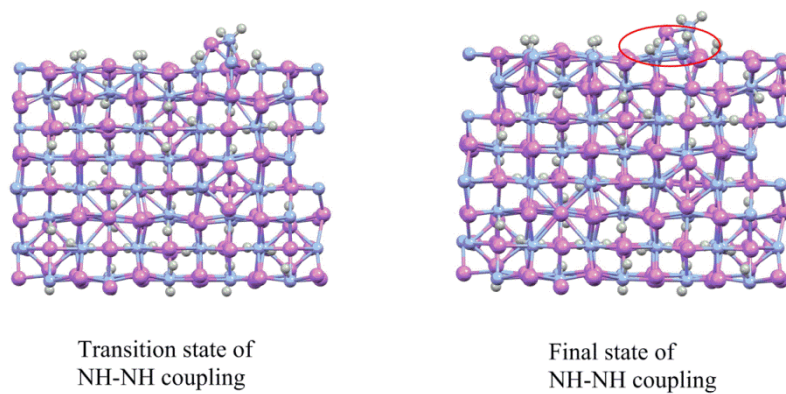


Figure S10. NH₃ reaction order α over 5 wt% Ru-LiNH₂ at different reaction temperatures. Reaction condition: sample loading – 30 mg, NH₃/Ar flow rate – 30 ml min⁻¹.

a)



b)



c)

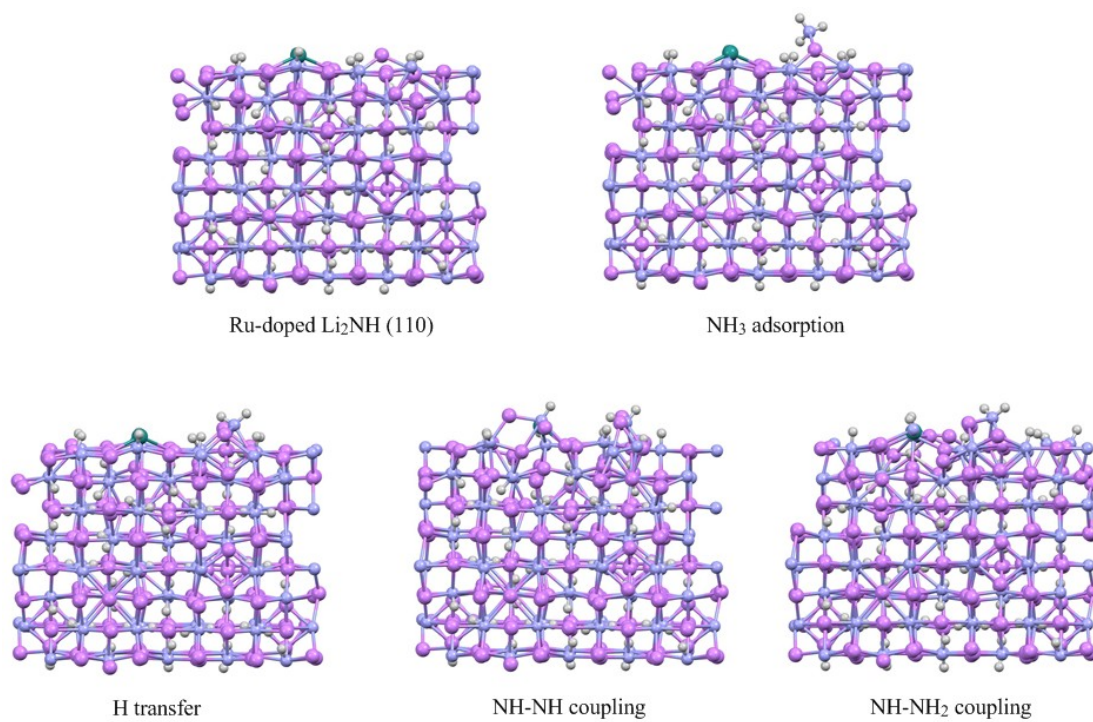


Figure S11. (a) Reaction pathway of NH_3 adsorption on the pristine and Ru-doped Li_2NH (110) surface and the follow-up NH-NH and NH-NH_2 coupling. The values in parentheses are the calculated energies for the Ru-doped Li_2NH surface. We did not simulate the $\text{NH}_2\text{-NH}_2$ coupling because of the less chance of occurrence. (b) The models of the transition state and final state of NH-NH coupling simulated from DFT calculations. (c) The models of Ru-doped Li_2NH , and NH_3 adsorption, H transfer, NH-NH coupling, $\text{NH}_2\text{-NH}_2$ coupling over Ru-doped Li_2NH (110) surface. Li, N, H and Ru atoms are represented as purple, light blue, grey and dark green spheres, respectively.

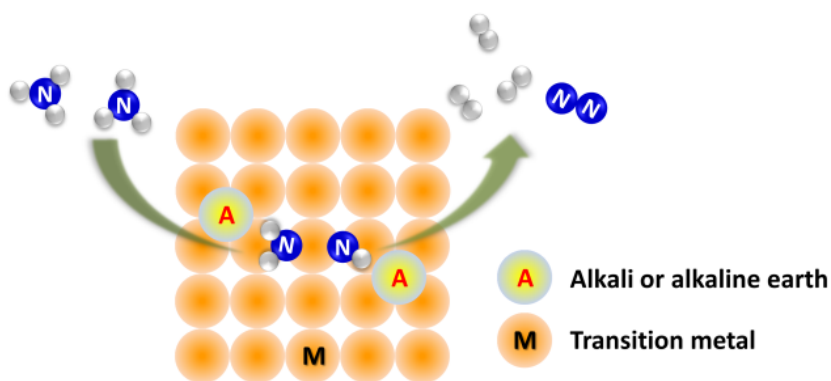


Figure S12. Scheme of NH_3 decomposition on alkali or alkaline earth metal amide – transition metal composites.

Reference

1. H. B. Guan, P. Wang, H. Wang, B. Y. Zhao, Y. X. Zhu and Y. C. Xie, *Acta Phys. Chim. Sin.*, 2006, **22**, 804-808.
2. S. F. Yin, B. Q. Xu, C. F. Ng and C. T. Au, *Appl. Catal. B*, 2004, **48**, 237-241.
3. S. F. Yin, B. Q. Xu, S. J. Wang, C. F. Ng and C. T. Au, *Catal. Lett.*, 2004, **96**, 113-116.
4. (a) G. Kresse and J. Hafner, *Phys. Rev. B*, 1993, **47**, 558-561; (b) G. Kresse and D. Joubert, *Phys. Rev. B*, 1999, **59**, 1758-1775.
5. P. E. Blochl, *Phys. Rev. B*, 1994, **50**, 17953-17979.
6. (a) J. P. Perdew, K. Burke and M. Ernzerhof, *Phys. Rev. Lett.*, 1996, **77**, 3865-3868; (b) J. P. Perdew, K. Burke and M. Ernzerhof, *Phys. Rev. Lett.*, 1997, **78**, 1396-1396.
7. H. J. Monkhorst and J. D. Pack, *Phys. Rev. B*, 1976, **13**, 5188-5192.